Coordinated Primary and Secondary Control with Frequency-Bus-Signaling for Distributed Generation and Storage in Islanded Microgrids

Wu, Dan; Tang, Fen; Dragicevic, Tomislav; Vasquez, Juan Carlos; Guerrero, Josep M.

Published in:
Proceedings of the 39th Annual Conference of the IEEE Industrial Electronics Society, IECON 2013

DOI (link to publication from Publisher):
10.1109/IECON.2013.6700319

Publication date:
2013

Document Version
Early version, also known as pre-print

This document is the preprint version of the paper:
D. Wu, T. Dragicevic, J.C. Vasquez, and J.M. Guerrero, "Coordinated primary and secondary control with frequency-bus-signaling for distributed generation and storage in islanded microgrids," in Proc. of the 39th Annual Conference of the IEEE Industrial Electronics Society, *IEEE IECON'13*, Vienna, Austria, Nov 2013.

Coordinated Primary and Secondary Control with Frequency-Bus-Signaling for Distributed Generation and Storage in Islanded Microgrids

Dan Wu[1], Fen Tang[1,2], Tomislav Dragicevic[1], Juan C. Vasquez[1], and Josep M. Guerrero[1]
[1] Department of Energy Technology, Aalborg University. Denmark
{dwu , tdr , juq , joz}@et.aau.dk
[2] School of Electrical Engineering, Beijing Jiaotong University, P. R. China
ftang_nego@126.com

***Abstract*— In this paper, a distributed coordinated control scheme based on frequency-bus-signaling (FBS) method for a low-voltage AC three phase microgrid is proposed. The control scheme is composed by two levels. Firstly a primary local control which is different for the DGs and the ESS is proposed. The ESS adopts FBS control which is based on changing slightly the bus frequency in the microgrid when the state-of-charge is near to the limit. This way, the DG controller when detecting that the frequency is increasing, will reduce the injected power by using a virtual inertia control loop. Then secondary control is implemented to restore the frequency deviation produced by the primary ESS controller while preserving the coordinated control performance. Real-time simulation results show the feasibility of the proposed approach by showing the operation of the microgrid in different scenarios.**

Keywords*— Coordinated control, virtual inertia, primary control, secondary control, droop control, frequency bus signaling, microgrids

I. INTRODUCTION

A Microgrid can be considered as a local grid with multiple distributed generators (DGs), energy storage systems (ESS), and loads, able to operate in either grid-connected or islanded modes, with seamless transition between both modes [1].

In grid connected mode of AC microgrid, the AC bus frequency and voltage are fixed by the main grid, and all the DGs are working as grid following units to exchange power with main grid. However in islanded mode, the power exchange among DGs, ESS and loads should be balanced inside the isolated microgrid. In the literature, the most popular control technique used in islanded microgrids is the droop method. It consists on adjusting the frequency of the inverters in function of output active power to achieve power sharing [2-4]. When using multilayer hierarchical control systems, this method is defined inside the primary local controllers [5]. Although this technique works well when we have fully dispatchable generators, such as uninterruptible power supply systems or energy storage integrated units, however when combining renewable energy sources (RESs) like photovoltaics (PV) or windturbines (WT) the dispatching is limited to the maximum power point tracking (MPPT) and is meaningless to get equal current sharing between RES and ESS. Further, ESSs have limitations in terms of state-of-charge (SoC) that have to be respected to avoid damages and failures. This means that when the SoC is near to the maximum, the power produced by the DG should be reduced to limit power of ESS. Consequently, in an islanded microgrid there is a need of coordination between DGs and ESS units.

To achieve the coordinated behavior among DGs and ESS, centralized controllers in energy management system (EMS) are proposed in [6-7]. In the literatures, the upper level controller makes decisions taking into account of SoC and give commands to local controllers. However, the drawback is that system stability relies on a microgrid central controller (MGCC) and its communication links [8]. If they are disabled, the whole system loses the coordination signal. To overcome the limitation of the centralized coordinated control, decentralized coordinated control can be implemented to enhance the system reliability. Among the control strategies, bus-signaling method (BSM) is a very promising way to implement since power line is used to transmit coordinated signals instead of using external fast communication links. In [9-10], BSM is used as power management among ESS, RESs and loads in DC systems. By changing the bus voltage according to different thresholds, the coordination signal is communicated to other units. However, this control law needs the modes changes among units, which makes the parameters of units hard to be designed and even may cause the unstable operation in the dynamic switching process.

In this paper, a frequency bus signaling (FBS) method is proposed for AC islanded microgrids. When the SoC of ESS is approaching high, the power of ESS is limited; at the same time the RESs operate in off-MPPT mode automatically. It is worth noticing that no modes changes is required in this method, thereby avoiding the dynamic stability problem may occur in previous BSM. The paper is organized as follows. Section II presents the system description, Section III gives the ESS and RESs control algorithms in primary level. In order to eliminate the AC bus frequency deviation produced in primary control, a secondary coordinated control is proposed in Section

IV. Section V gives the detailed description of control implementation of ESS and RESs, and finally the real-time simulation results are presented in Section VI to validate the proposed control strategy.

II. MICROGRID SYSTEM DESCRIPTION

Fig.1 shows a flexible microgrid consists of RESs and ESS with batteries which can operate in either grid connected mode or islanded mode according to the state of Intelligent Bypass Switch (IBS). To make the maximum utilization of renewable energy, the RESs usually operate in MPPT as grid following units in both grid connected mode and islanded mode. However, the roles of ESS are different in each operating mode. In grid connected operation, the behavior of ESS should be determined by both its SoC and time of use (TOU) of electricity. This means that besides discharging the power to supply loads, the ESS can also take additional function as peak shaving in peak period of grid. While in islanded operation, the ESS usually works as grid forming unit to maintain the common grid bus. Since islanded microgrid has no power exchange with main grid, the ESS also has to operate as energy buffer to balance the power between sources and loads. Therefore, to obtain a reliable energy management function among RESs, ESS and loads, the capability of ESS based on SoC is very important when coordinate various units in islanded microgrid. The following description is based on the analysis of islanded microgrid operation.

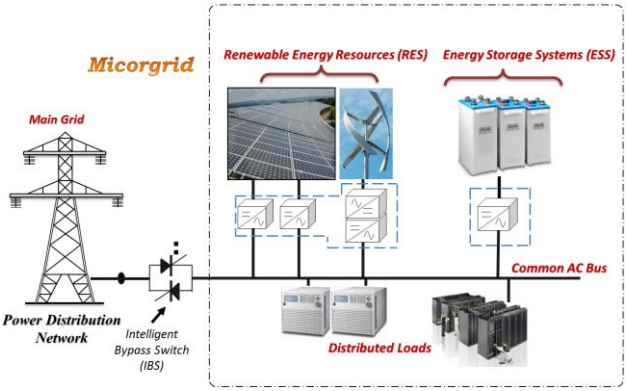

Fig. 1. Microgrid system desctription

III. PRIMARY COORDINATED CONTROL

The primary control in microgrid is developed aimed at regulating the output power of each unit, at the same time maintaining the stability of bus voltage and frequency. Usually, the ESS and RESs units are controlled as master-slave way as Fig. 2 presented. The ESS works as master unit maintaining AC bus voltage E^* and frequency f^*, and RESs operate as slave units regulating its output power according to MPPT.

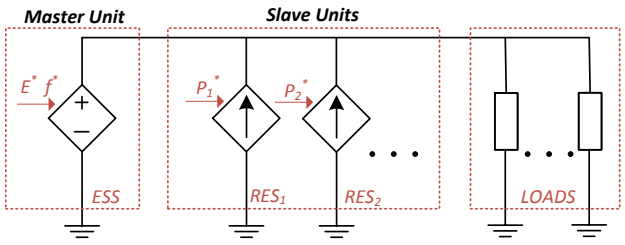

Fig. 2. Master-slave control of islanded microgrid

In order to obtain a coordinated control among units according to SoC and MPPT, the system control structure based on FBS is proposed in Fig. 3. The coordinated control strategy can be classified into primary local level and secondary centralized level. In the primary level, there is no need of communication among ESS and RESs units. According to estimated SoC, the ESS changes the bus frequency as signaling, and RESs receive the signaling in AC bus to change the output power. However the frequency deviation will result in this level. Then if requirement for the tight frequency range is needed, additional secondary control level can be applied to restore frequency in nominal value with low bandwidth communication link, which will be illustrated in section IV. In this part, the primary control level is illustrated based on ESS master control and RES slave control respectively.

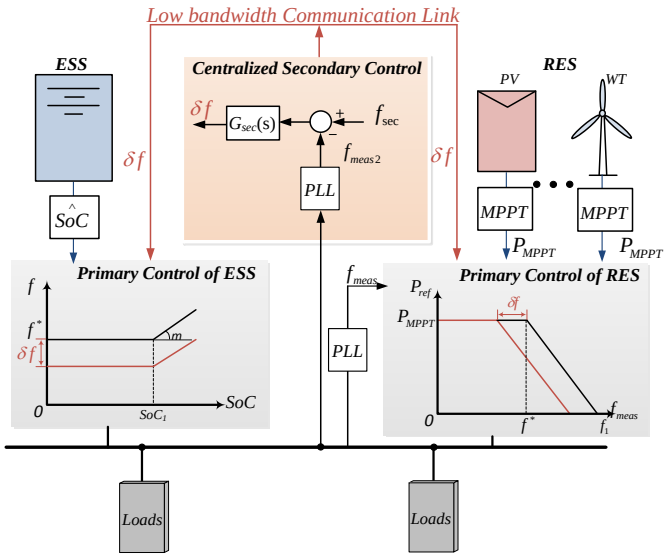

Fig. 3. Coordinated control structure

A. ESS Master Control-Bus Signaling Control.

In [3], it has been illustrated that when the output impedance of converter is highly inductive, the active power can be controlled almost exclusively by the output frequency. Therefore, it makes sense using frequency of ESS as signal to coordinate units when SoC approaching high.

Fig. 4 shows the diagram of ESS frequency signaling. f^* and f_1 are the normal frequency and maximum frequency, and SoC_1 is the SoC threshold of ESS. f_e and SoC_e are the final value of frequency and SoC. When SoC is lower than the up threshold, the ESS regulates its output frequency as nominal value. When SoC is higher than the threshold, the frequency then increases with slope of m to coordinate other units to maintain SoC. The output frequency of ESS is determined as

$$\begin{cases} f = f^* & SoC \le SoC_1 \\ f = f^* + m\cdot(SoC - SoC_1) & SoC > SoC_1 \end{cases} \quad (1a)$$

where the boost frequency coefficient m can be defined as

$$m = \frac{f_1 - f^*}{100\% - SoC_1} \quad (1b)$$

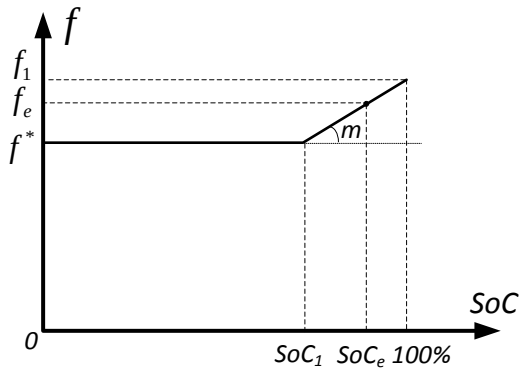

Fig. 4. Frequency signalling of ESS

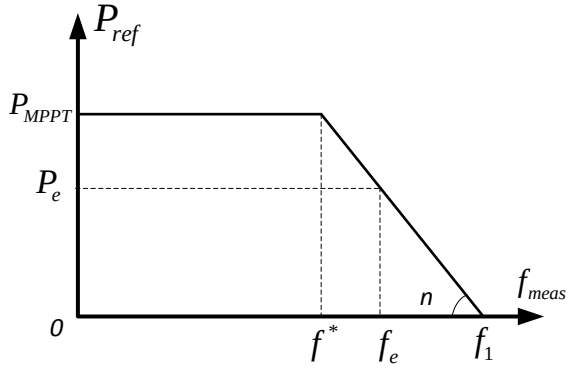

Fig. 5. Virtual inertia of RES

B. RES Slave Control-Virtual Inertia Control.

Having the frequency increasing, each RES unit decreases power from maximum power point. This performance is similar with the inertia response of the power system. In this case, the power drop of RESs may be achieved by adding virtual inertia of system. Fig. 5 shows the virtual inertia performance of RESs, where P_{ref} is the active power reference of RESs, P_{MPPT} and P_e referred to the MPPT point and final power output of each RESs, and f_{meas} is the sensing frequency by the phase lock loop (PLL). When the f_{meas} not above nominal frequency, RES units are working under MPPT state, and making the full use of renewable energy. When f_{meas} is above f^*, RES units start to decrease output power to limit SoC of ESS coordinately. As the frequency reflects the SoC information, the higher is the bus frequency, the lower is the power from RESs. Finally, when the power absorbed by the ESS is low enough to maintain SoC, the frequency will be stable at f_e, and power from RES unit has decreased to P_e. Thus the active power reference of each RES can be expressed as following

$$\begin{cases} P_{ref} = P_{MPPT} & f_{meas} \le f^* \\ P_{ref} = P_{MPPT} - n\cdot(f_{meas} - f^*) & f_{meas} > f^* \end{cases} \quad (2a)$$

where the virtual inertia coefficient n can be defined as

$$n = \frac{P_{MPPT}}{f_1 - f^*}. \quad (2b)$$

Usually the microgrid frequency is measured by the RES by means of PLL, which can be approximated as a first order system [11]. Hence, the measured frequency f_{meas} can be expressed as

$$f_{meas} = \frac{1}{\sigma s + 1} f \quad (3)$$

where σ is the time constant of the PLL.

Considering that the system is working in the condition $SoC_1<SoC<100\%$, and from (1) and (2), the RES power reference takes the form

$$P_{ref}(s) = P_{MPPT} + \frac{n\sigma}{\sigma s + 1}\dot{f} - n\cdot m(SoC - SoC_1) \quad (4)$$

whereas $\dot{f}$ denotes the differential of frequency .

Consequently, using small-signal analysis the closed-loop system inertia can be calculated according to the following definition [12]

$$G_{vi}(s) \triangleq \frac{\Delta P_{ref}(s)}{\Delta \dot{f}(s)} = \frac{n\sigma}{\sigma s + 1} \quad (5)$$

It can be seen that when n is limited by the maximum frequency deviation, tuning independently the time constant σ can change the inertia response of the RESs.

IV. SECONDARY COORDINATED CONTROL

As previous analyzed, the bus signaling of ESS with only primary control results in frequency deviation. Although this frequency deviation can be designed inside the allowable limits, but some events like reconnection to main grid or synchronous machines connection to the microgrid may require tight frequency regulation. The aim of this Section is to propose a secondary control to cancel the frequency deviation produced by the primary control, while preserving the autonomous operation of each unit.

Fig. 6 shows the bus signal method of ESS with the secondary control action. When $SoC > SoC_1$, the *f–SoC* curve of the ESS shifts downwards in order to regulate the microgrid frequency in steady state. Then, we can modify the control strategy (1) by adding a shifting-frequency term, thus (1) can be rewritten as

$$\begin{cases} f = f^* & SoC \le SoC_1 \\ f = f^* + \delta f + m\cdot(SoC - SoC_1) & SoC > SoC_1 \end{cases} \quad (6)$$

where δf is the shifting-frequency term, which adjust (6) to achieve $f=f^*$ anytime. The secondary control will generate δf by using the following centralized PI controller:

$$\delta f = G_{\sec}(s)\cdot(f_{\sec} - f_{meas2}) = \left(k_{p\sec} + \frac{k_{i\sec}}{s}\right)\cdot(f_{\sec} - f_{meas2}) \tag{7}$$

where k_{psec} and k_{isec} are the proportional and integral terms, respectively; f_{sec} is the secondary frequency reference; f_{meas2} is the measured frequency obtained by secondary control PLL, which can be as in (3) approximated by the following first order approximation:

$$f_{meas2} = \frac{1}{\sigma_2 s + 1} f \tag{8}$$

where σ_2 is the time constant of the PLL of secondary control.

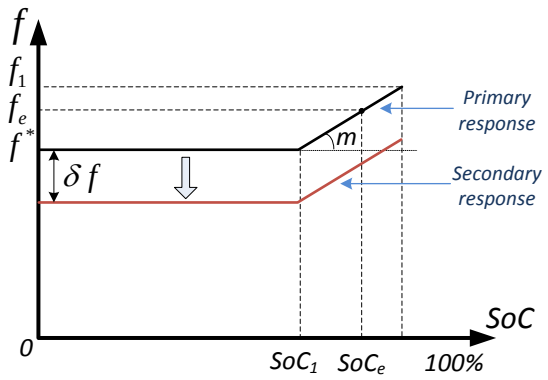

Fig. 6. Secondary control action over the frequency signalling of ESS.

On the other hand, if we restore the frequency in the microgrid, then the effect of the RES primary control will be cancelled, so that we need to change the frequency threshold of equation (2), which can be modified as following:

$$\begin{cases} P_{ref} = P_{MPPT} & f_{meas} \le f^* + \delta f \\ P_{ref} = P_{MPPT} - n\cdot(f_{meas} - f^* - \delta f) & f_{meas} > f^* + \delta f \end{cases} \tag{9}$$

Notice that now the frequency threshold, instead of just using f^* now also incorporates the shifting-frequency term δf. Fig 7 shows the adaptive behavior of the frequency threshold changing for the virtual inertia function. Consequently, the RESs will deliver the output power commanded by P_{ref}, coordinated with the bus signaling but without frequency deviation.

For coherency, the secondary frequency reference is selected as $f_{sec} = f^*$, then by combining (6) and (9), we can obtain the power reference dynamics of RESs:

$$P_{ref}(s) = P_{MPPT} + \frac{n\sigma}{\sigma s + 1}\dot{f} - nm(SoC - SoC_1) \tag{10}$$

So that, from (10) the closed-loop system inertia with secondary control can be calculated as:

$$G_{vi}(s) \triangleq \frac{\Delta P_{ref}(s)}{\Delta \dot{f}(s)} = \frac{n\sigma}{\sigma s + 1} \tag{11}$$

It can be seen that the secondary control can be used to restore the bus frequency without changing the local inertia response of RESs.

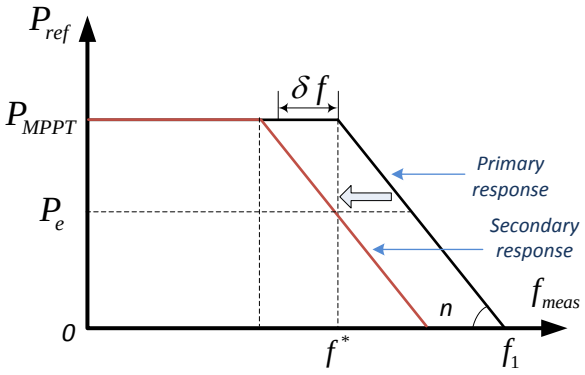

Fig. 7. Virtual inertia control of RESs with secondary control

V. Control Implementation

The aim of this section is to illustrate the control implementation in details for each of the control loops previously proposed. The control algorithm is shown in Fig. 8.

A. Inner control loops

The inner loops are designed to control the output voltages and currents of each unit. For ESS, it operates as grid forming unit in voltage control mode (VCM) and regulate the output frequency and voltage according to primary control commands. For RESs, they operate as grid following units in current control mode (CCM) to regulate its output currents according to primary control commands with phase lock loop (PLL). To obtain a good transient and steady state performance similar with DC system, both ESS and RESs employ PI controllers implemented in *d-q* synchronous reference frame with *abc-dq* reference frame transformation.

B. Primary ESS control

The objective of primary ESS control is to change the frequency of voltage reference according to the estimated SoC. When estimated SoC above the threshold, the frequency is changed steadily based on (1a). And the slope of *m* is designed according to maximum frequency deviation as (1b).

C. Primary RES control

The primary RES control is aimed at changing the output power of each RES unit according to the bus frequency signaling from ESS. When detecting the bus frequency above the nominal value, the output power is changed with (2a). Also the inertias of RESs are designed with respect to different time constant of PLL and slope *n* according to (4). Hence, by changing the output power of each RES, the power dispatching of system changed, and the power flow into ESS can be limited.

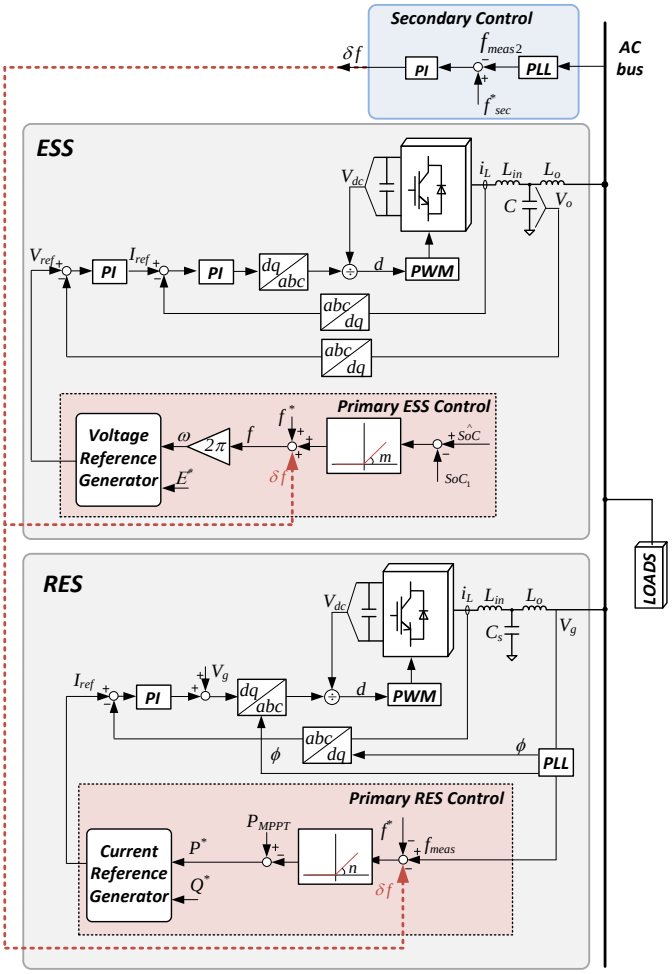

Fig. 8. Control algorithm of ESS and RES

D. Secondary control

The secondary control of whole system is to eliminate the final frequency deviation when SoC approaching limitation. It is achieved by using (6) and (9), thereby changing the frequency deviation setpoint of ESS and RESs. It should be noted that the secondary control is optional in system since the coordinated control of system is achieve in primary level even without communication. Then if the islanded microgrid is required in advance situation like synchronized with main grid, this secondary control with low bandwidth can be used in addition.

TABLE I. POWER STAGE PARAMETERS

Item	Symbol	Value
Nominal output voltage	E	230 V
Nominal output frequency	f^*	50 Hz
Filter inductor	L_{in}	1.8 *mH*
Output inductor	L_o	1.8 *mH*
Output capacitor of ESS	C	27 μF
Output capacitor of RES	C_s	4.7 μF
Power of Loads	P_L	1.6 *kW*

TABLE II. COORDINATED CONTROL PARAMETERS

Item	Symbol	Value
Microgrid frequency threshold	f_1	51Hz
SoC upper limit	SoC_1	95%
Secondary frequency reference	f_{sec}	50Hz
Secondary control proportional term	$k_{p\,sec}$	0.005
Secondary control Integral term	$k_{i\,sec}$	0.5 s^{-1}
Time constant of RES PLL	σ	0.56 s

VI. REAL-TIME SIMULATION RESULTS

The proposed coordinated control strategy is validated through real-time simulation based on dSPACE platform. The described system is composed of one ESS and two RES units. The power stage parameters of ESS and RESs are shown in Table I, the control parameters are shown in Table II.

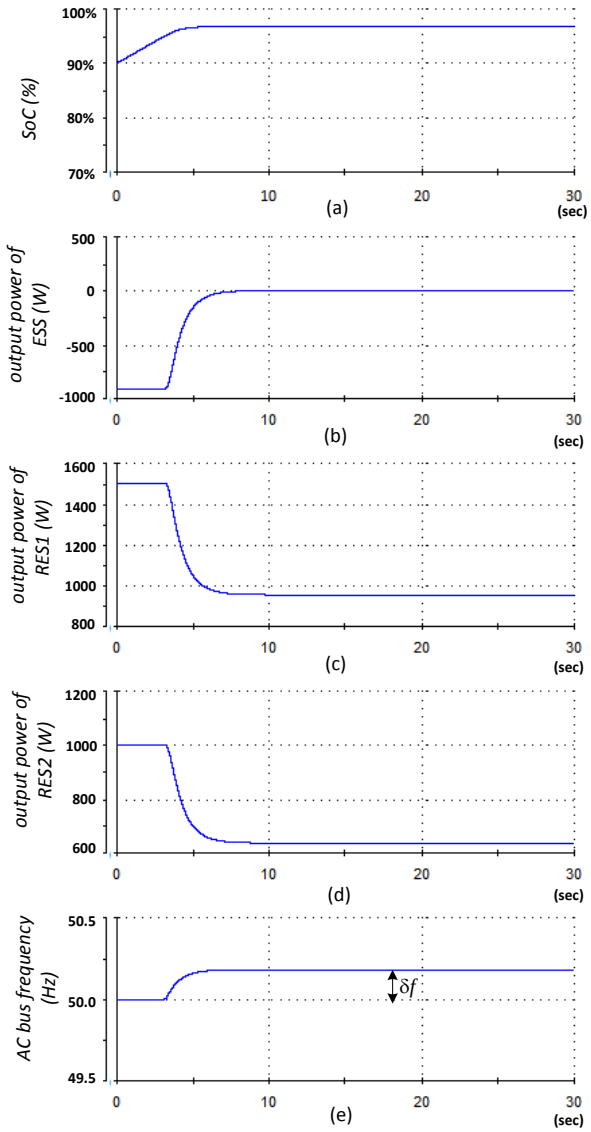

Fig. 9. Simulation results of primary coordinated control

Fig.9 shows the simulation results with only primary coordinated control. Before the ESS is approaching the charging limitation 95% of SoC, ESS operates as VCM, and the RESs are operating as ideal current controlled mode with output power of 1.5kW and 1kW. When SoC is over the charging threshold 95% as shown in Fig. 9(a), then primary coordinated control is activated, the input power of ESS starts to be limited in Fig. 9(b) by coordinated decrease the output power of RESs in Fig.9(c) and Fig. 9(d). Finally, the input power of ESS can be limited to almost zero to maintain its SoC. And as shown in Fig. 9(e), there is a frequency deviation about 0.2Hz of AC bus frequency in steady state.

The simulation results adding secondary control is presented in Fig.10. When SoC is over the charging threshold 95% as shown in Fig. 10(a), not only the primary control is activated, but also the secondary control is enabled to restore frequency. Compared to Fig. 9(e), Fig. 10(e) shows that with secondary control, the AC bus frequency can be restored to 50 Hz with secondary coordinated control.

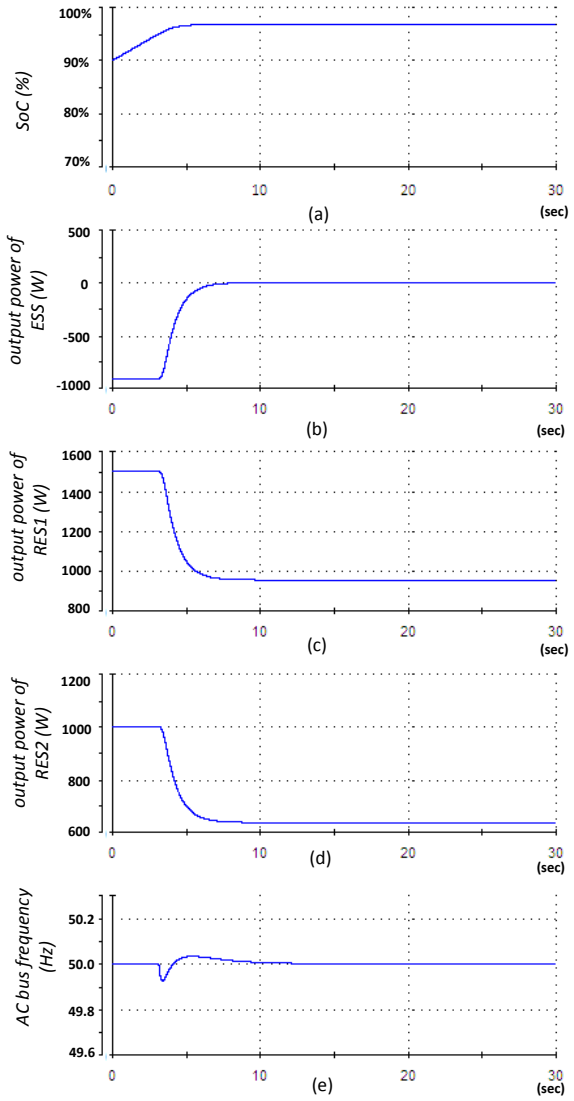

Fig. 10. Simulation results of secondary coordinated control

VII. Conclusion

This paper gave a distributed coordinated control strategy among DGs and ESS in islanded microgrid based on frequency bus signaling method. In the proposed control strategy, the primary control is used based on FBS of ESS and virtual inertia response of RESs to achieve the power balancing among ESS and RESs in different SoC condition of ESS. Thus the ESS can be prevented from overcharging by the primary coordinated control. To eliminate frequency deviation, a centralized secondary control was implemented without changing the coordinated control behavior of primary control. The simulation results have validated the proposed control strategy in both primary and secondary level.

References

[1] IEEE Guide for Design, Operation, and Integration of Distributed Resource Island Systems with Electric Power Systems," *IEEE Guide for Design, Operation, and Integration of Distributed Resource Island Systems with Electric Power Systems*.

[2] Tuladhar, A.; Hua Jin; Unger, T.; Mauch, K., "Control of parallel inverters in distributed AC power systems with consideration of line impedance effect," *Industry Applications, IEEE Transactions on* , vol.36, no.1, pp.131,138, Jan/Feb 2000

[3] Alves Coelho, E.A.; Cortizo, P.C.; Garcia, P.F.D., "Small signal stability for single phase inverter connected to stiff AC system," *Industry Applications Conference, 1999. Thirty-Fourth IAS Annual Meeting. Conference Record of the 1999 IEEE* , vol.4, no., pp.2180,2187 vol.4, 1999

[4] Chandorkar, M.C.; Divan, D.M.; Adapa, R., "Control of parallel connected inverters in standalone AC supply systems," *Industry Applications, IEEE Transactions on* , vol.29, no.1, pp.136,143, Jan/Feb 1993

[5] Guerrero, J.M.; Chandorkar, M.; Lee, T.; Loh, P.C., "Advanced Control Architectures for Intelligent Microgrids—Part I: Decentralized and Hierarchical Control," *Industrial Electronics, IEEE Transactions on* , vol.60, no.4, pp.1254,1262, April 2013

[6] Olivares, D.E.; Canizares, C.A.; Kazerani, M., "A centralized optimal energy management system for microgrids," *Power and Energy Society General Meeting, 2011 IEEE* , vol., no., pp.1,6, 24-29 July 2011

[7] Jong-Yul Kim; Seul-Ki Kim; Jin-Hong Jeon, "Coordinated state-of-charge control strategy for microgrid during islanded operation," *Power Electronics for Distributed Generation Systems (PEDG), 2012 3rd IEEE International Symposium on* , vol., no., pp.133,139, 25-28 June 2012

[8] Tan, K.T.; Peng, X. Y.; So, P. L.; Chu, Y.C.; Chen, M. Z Q, "Centralized Control for Parallel Operation of Distributed Generation Inverters in Microgrids," *Smart Grid, IEEE Transactions on* , vol.3, no.4, pp.1977,1987, Dec. 2012

[9] Schonberger, J.; Duke, R.; Round, S.D., "DC-Bus Signaling: A Distributed Control Strategy for a Hybrid Renewable Nanogrid," *Industrial Electronics, IEEE Transactions on* , vol.53, no.5, pp.1453,1460, Oct. 2006

[10] Vandoorn, T.L.; Renders, B.; Degroote, L.; Meersman, B.; Vandevelde, L., "Active Load Control in Islanded Microgrids Based on the Grid Voltage," *Smart Grid, IEEE Transactions on* , vol.2, no.1, pp.139,151, March 2011

[11] Vasquez, J.C.; Guerrero, J.M.; Savaghebi, M.; Teodorescu, R., "Modeling, analysis, and design of stationary reference frame droop controlled parallel three-phase voltage source inverters," *Power Electronics and ECCE Asia (ICPE & ECCE), 2011 IEEE 8th International Conference on* , vol., no., pp.272,279, May 30 2011-June 3 2011

[12] Kundur P.; Power system stability and control. Tata McGraw-Hill Education, 1994.